PRESSURE AND VELOCITY MEASUREMENTS IN A THREE DIMENSIONAL WALL JET

By

G. D. Catalano
J. B. Morton
R. R. Humphris

April 9, 1978

(NASA-CR-157918) PRESSURE AND VELOCITY MEASUREMENTS IN A THREE DIMENSIONAL WALL JET (Virginia Univ.) 35 p HC A03/MF A01 CSCL 01A

N79-12011

Unclas
G3/02 32303

Backup Document for AIAA Synoptic Scheduled for Publication in the AIAA Journal, February 1979

University of Virginia
Department of Mechanical and
Aerospace Engineering
Charlottesville, Virginia 22901

SYNOPTIC BACKUP DOCUMENT

This document is made publicly available through the NASA scientific and technical information system as a service to readers of the corresponding "Synoptic" which is scheduled for publication in the following (checked) technical journal of the American Institute of Aeronautics and Astronautics.

- [XX] AIAA Journal, February
- [ ] Journal of Aircraft
- [ ] Journal of Spacecraft & Rockets
- [ ] Journal of Hydronautics

A Synoptic is a brief journal article that presents the key results of an investigation in text, tabular, and graphical form. It is neither a long abstract nor a condensation of a full length paper, but is written by the authors with the specific purpose of presenting essential information in an easily assimilated manner. It is editorially and technically reviewed for publication just as is any manuscript submission. The author must, however, also submit a full backup paper to aid the editors and reviewers in their evaluation of the synoptic. The backup paper, which may be an original manuscript or a research report, is not required to conform to AIAA manuscript rules.

For the benefit of readers of the Synoptic who may wish to refer to this backup document, it is made available in this microfiche (or facsimile) form without editorial or makeup changes.

PRESSURE AND VELOCITY MEASUREMENTS IN A THREE DIMENSIONAL WALL JET +

By

G. D. Catalano
J. B. Morton
R. R. Humphris

+Work Supported in part by NASA Grant No. NGR 47-005-219-3 and NSF Grant No. 7522488.

ABSTRACT

In three recent papers,[1-3] some results of an experimental investigation of a freely expanding coflowing jet as well as a three dimensional wall jet have been presented. A flat plate as well as a curved wall surface intended to model a wing-flap combination in a high lift V/STOL configuration have been investigated. In these papers, the ratio of the jet exit plane velocity to the free stream velocity, λ_j, was 5.1.

This paper explores the effects of increasing the velocity ratio, λ_j. The quantities measured include the width of the mixing region, the mean velocity field, turbulent intensities and time scales.
In addition, wall and static pressure-velocity correlations and coherences are presented.

The velocity measurements are made using a laser Doppler velocimeter (LDV) with a phase-locked loop processor. The fluctuating pressures are monitored using condenser-type microphones.

I. INTRODUCTION

One of the present designs being investigated for increasing the lifting capabilities of aircraft is termed Upper Surface Blowing. The exhaust gases of the jet engine are directed along the upper surface of the wing and,becoming attached,are turned by the wing's upper surface and trailing edge flaps. It has been found that a significant increase in lift is realized but the loading that the structure must endure is greatly increased. Hence, there exists a need for more information about the flow field for this "three dimensional wall jet."

Several previous reports [(1)-(3)] have dealt with the experimental investigation of the near field region of a three dimensional wall jet (Figure 1). The first report dealt with the one point statistical properties of the flow exiting the nozzle without any confining surfaces present. The vortex shedding model of a turbulent jet was clearly reinforced by the appearance of peaks in the velocity spectra in the potential core region of the flow.

The effects on the flow field of the axisymmetric jet of placing a flat wall surface, referred to as the plate, and a wall surface with large curvature, the flap, adjacent to the lip of the nozzle were the subject of the second report (C. F. Fig2a). It was found that the curved wall surface served to break up the potential core region of the jet much more rapidly than was the case for either the unconfined flow or the flow over the flat wall.

In the third paper, emphasis was placed on obtaining space-time correlations in the different turbulent flow fields from which iso-correlation contour maps were constructed. The iso-correlation contours for the turbulent flow fields demonstrate the existence of large-scale structures. The shape of the contours was significantly different for each of the three flow configurations in both the longitudinal and horizontal cross-sectional views. The contours depended on whether or not a confining surface was present and

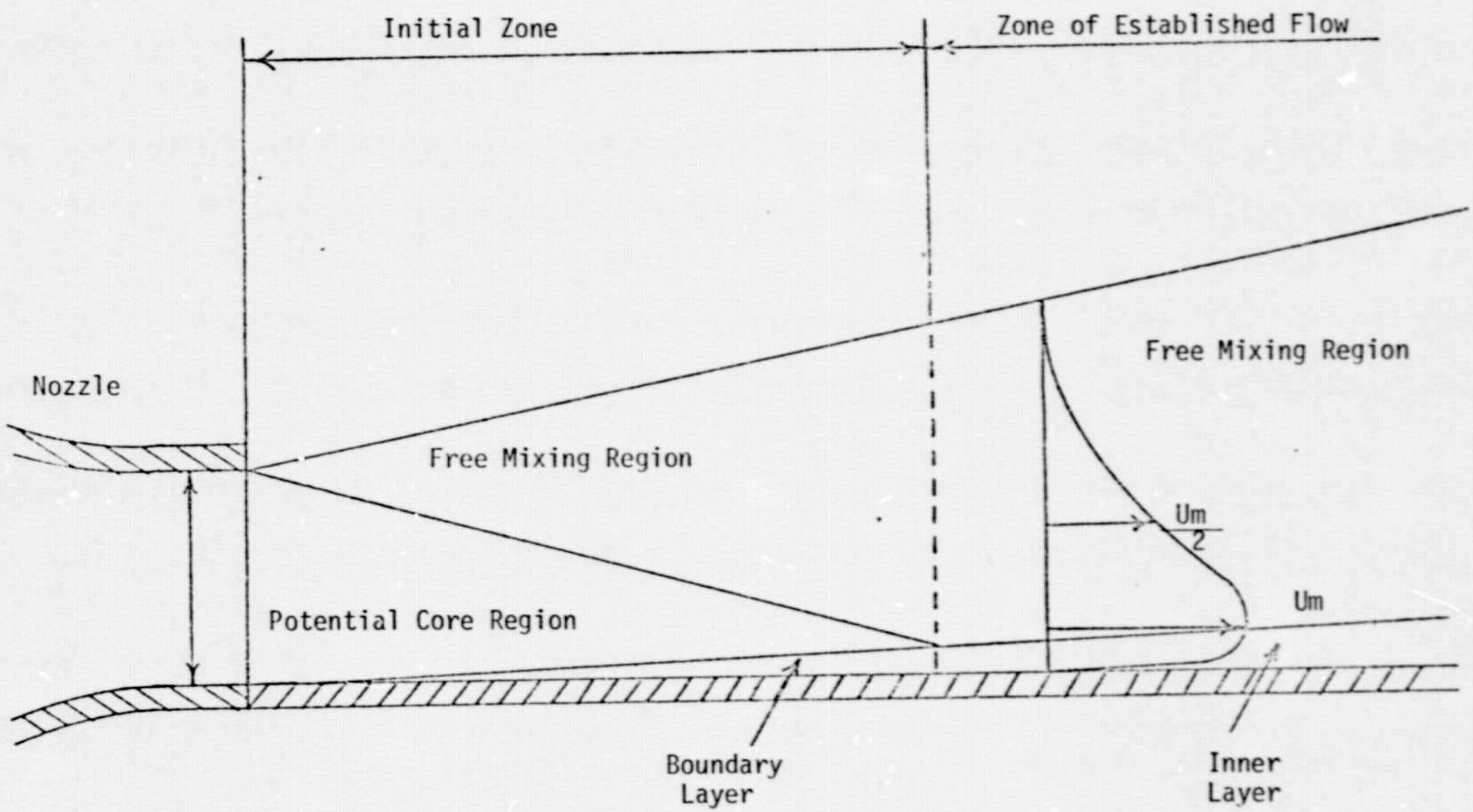

Figure 1 Schematic of a Wall Jet

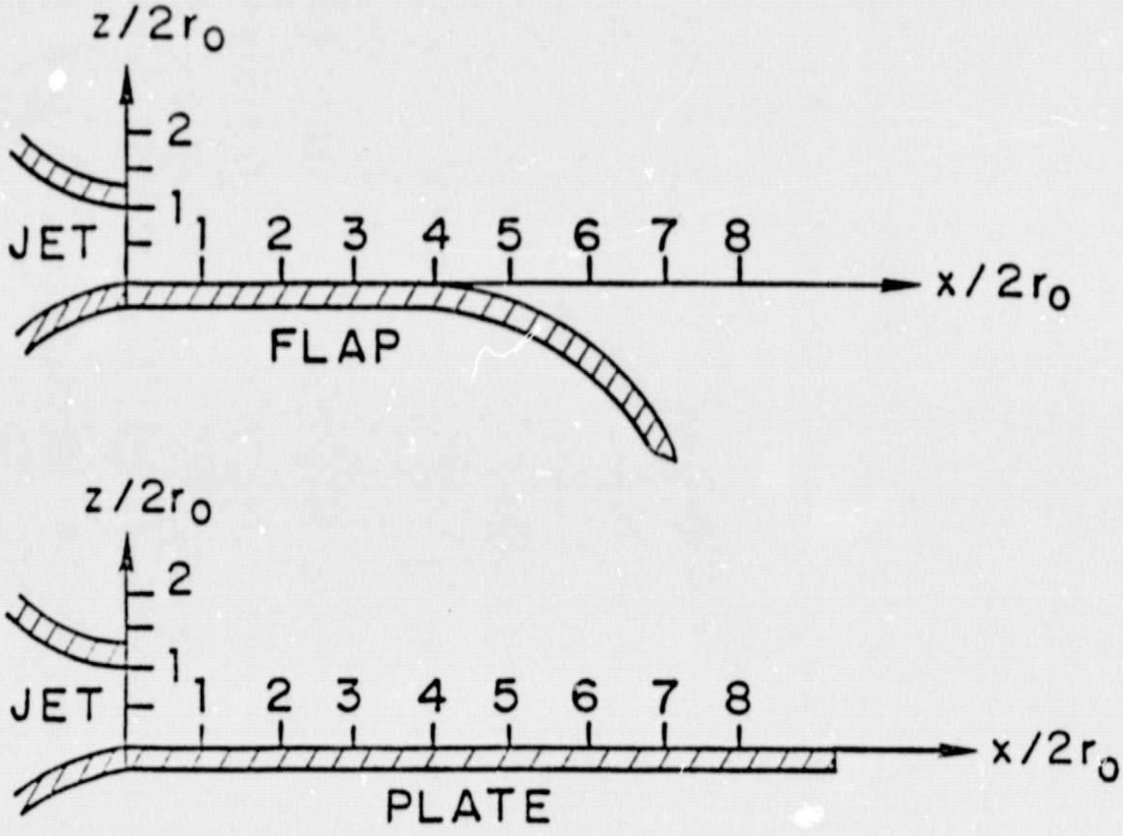

Figure 2(a) Flow Configurations

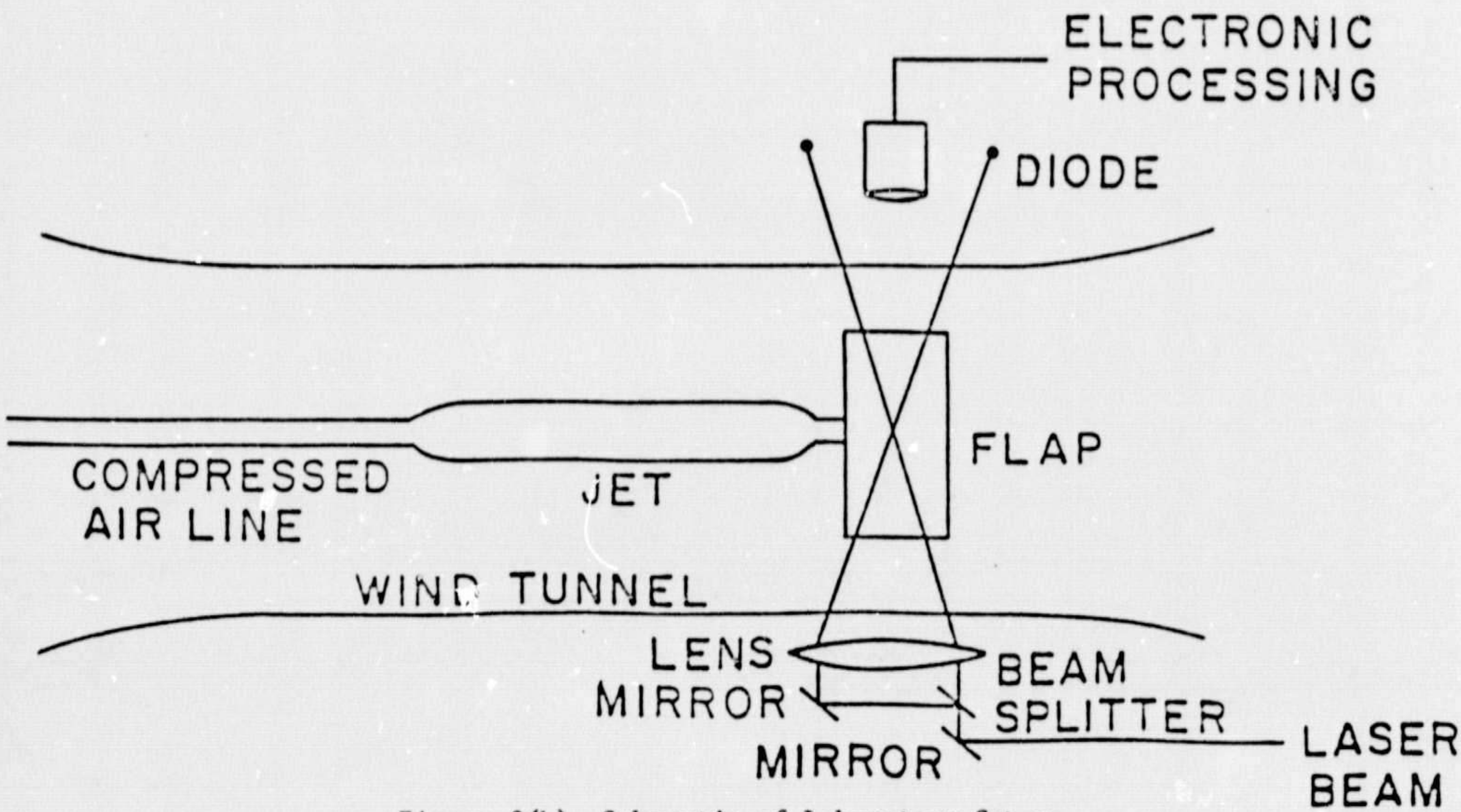

Figure 2(b) Schematic of Laboratory Set-up whether the wall was flat or curved.

The present paper has two main emphasis. First, the effects on the flow fields of varying the ratio of the velocity at the exit plane of the nozzle to the outer tunnel flow are reported. Second, pressure-velocity correlations are taken and some trends are discussed. Emphasis is placed on comparing the coherence between the fluctuating pressure and velocity fields at various locations in the different flow configurations.

The same three flow fields investigated in the second and third reports[2-3] are studied here. The arrangement of the confining surfaces, the flap and the flat plate are shown in Figure 2(a) and a schematic of the whole facility is shown in Figure 2(b).

II. EXPERIMENTAL EQUIPMENT AND TECHNIQUES

A two-color laser Doppler velocimeter in conjunction with a phase locked-loop processor is used to make the velocity measurements. The two strongest frequencies of an argon ion laser in the "all lines" mode of operation are selected for use. The two-color LDV system allows the velocity at two different points in the flow fields to be determined with displacement between the probes possible in all three directions. This system is described in more detail in reference 1.

To determine the static and wall surface pressures, the system developed by Schroeder[4] and Herling[5] is used. The essential items include a 1/2 inch condenser-type microphone and a tape recorder. When cross-correlations are made between the fluctuating pressure and velocity fields, both signals are filtered (10Hz - 1000Hz) before being processed in order to achieve a good signal-to-noise ratio.

A computer program is used that enables the spectra of both the pressure and velocity to be obtained as well as the coherence between the two signals. Coherence is essentially the value of the cross-correlation coefficient as a function of frequency. If G_{11} and G_{22} denote the Fourier Transform of the autocorrelation function of pressure and velocity repectively, then the coherence, δ_{12}^2, is defined as follows:

$$\delta_{12}^2 = \frac{|G_{12}|^2}{G_{11}G_{22}}$$

where G_{12} represents the Fourier Transform of the cross-correlation function between the pressure and velocity fluctuations.

III. EXPERIMENTAL RESULTS

A. Mean Velocity Field

The effects of the velocity ratio, λ_j, on the width and decay of the centerline velocity for the three respective mean flow fields are presented in Figures 3 and 4. In Figures 3(a) and (b) for $\lambda_j = 5.1$ and 10.88, the non-dimensionalized mixing width, $y_m/2r_o$ is plotted versus $x/2r_o$ for $z/2r_o = 0.5$. The quantity, y_m, is defined as the lateral distance from the centerline to the location where the mean velocity is the arithmetic average of its value on axis and in the secondary stream. The results are compared to a theoretical curve developed by Squire and Trouncer[6].

First, consider the findings for $\lambda_j = 5.1$. While the agreement between the theoretical curve and experimental results for the coflowing jet is quite good, one effect of the confining surfaces can be seen. For the flow over the flap, the value of $y_m/2r_o$ increases much more rapidly than is the case for the other two configurations. With the plate in place, however, the value of $y_m/2r_o$ is somewhat smaller than that for the coflowing jet for the first several diameters downstream but eventually is comparable in magnitude. For $\lambda_j = 10.88$, the results are less clear. However, the rate of increase of $y_m/2r_o$ is considerably less for the flap than is the case for $\lambda_j = 5.1$. It is difficult to draw any strong conclusions, however, since the data is somewhat sketchy. Here, also the mixing widths of the unconfined jet and flow over the plate are comparable in magnitude.

In Figures 4(a) and (b), the decay of the centerline mean velocity at $z/2r_o = 0.5$ for varying downstream locations is presented. In these Figures, U_o is the centerline velocity and U_{FS} is the secondary (wind tunnel) velocity. The meaning of the data for the two jet/confining surface configurations should be discussed. As the flow exits the circular nozzle, the plate and flap

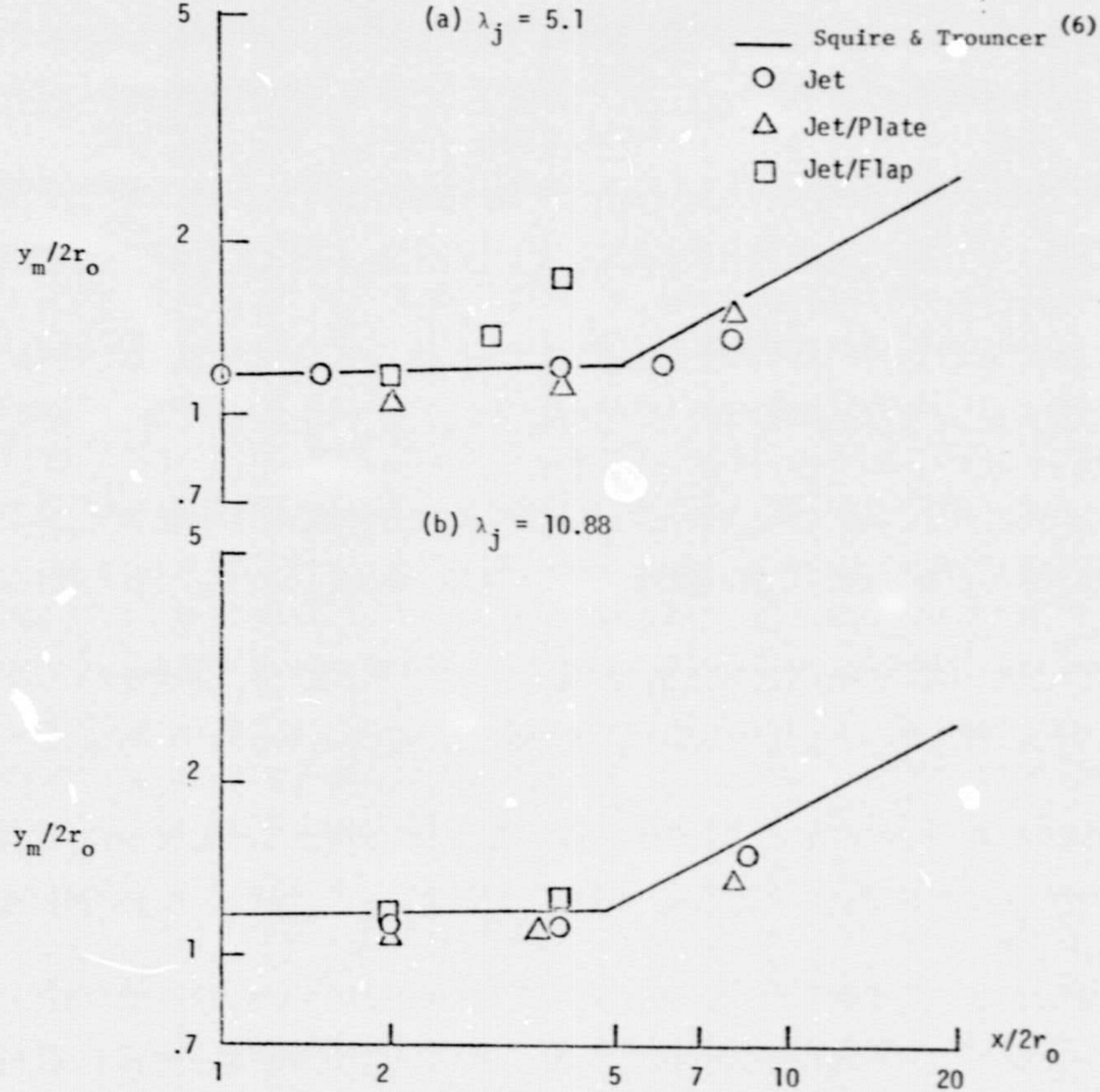

Figure 3 Growth of Mixing Width

(a) λ_j = 5.1

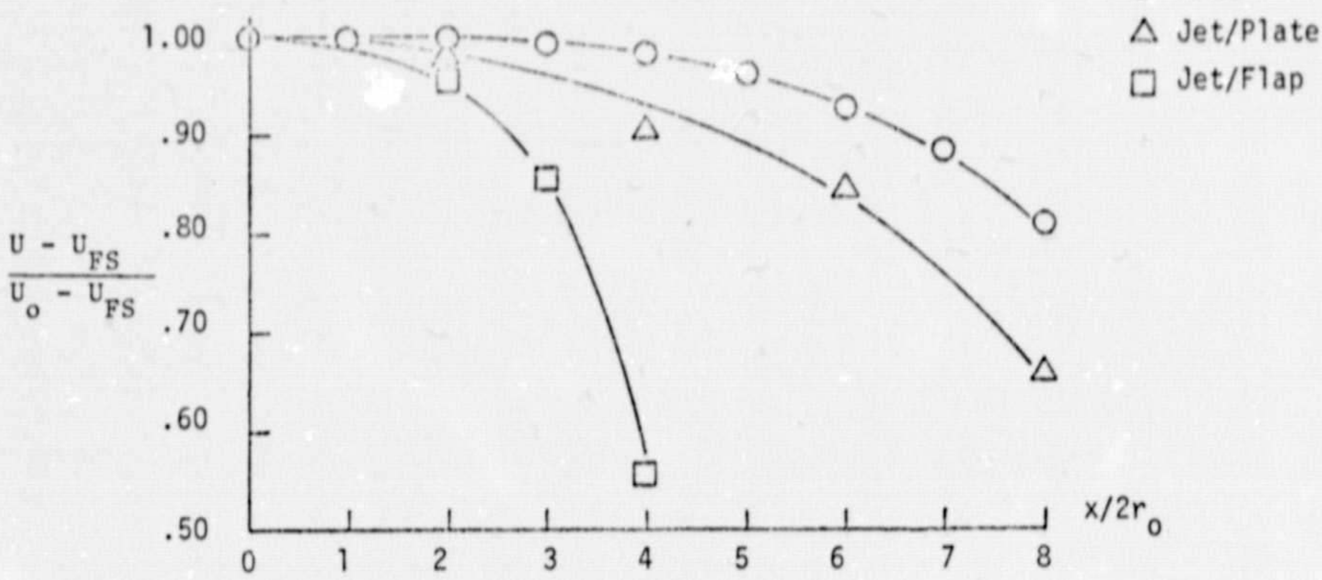

(b) λ_j = 10.88

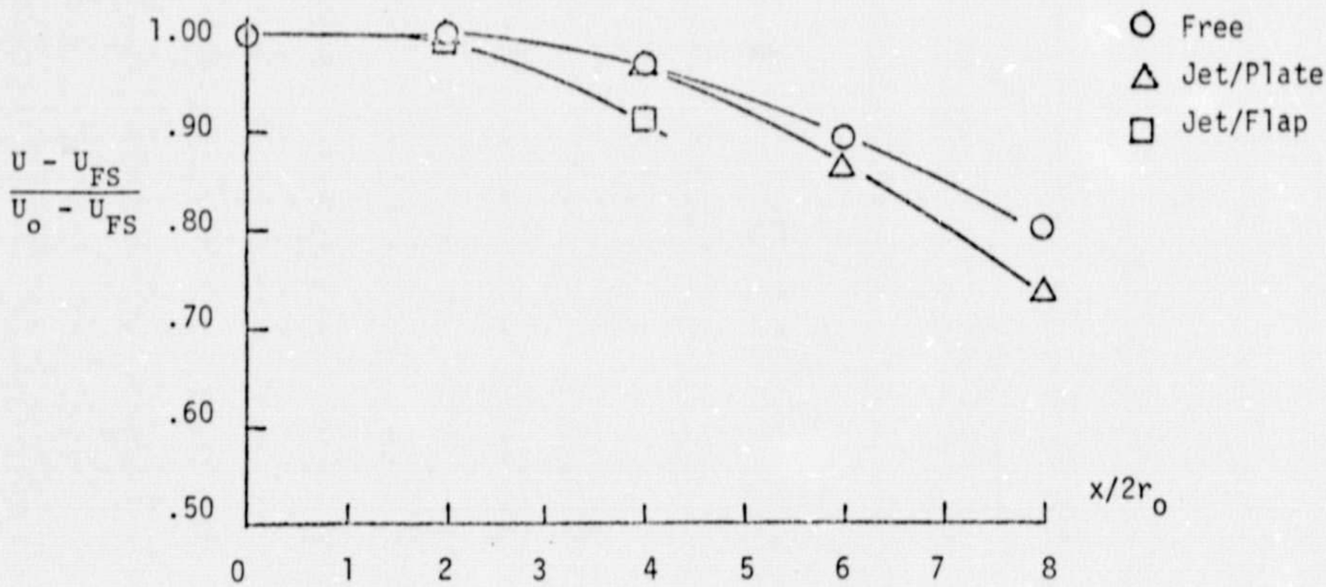

Figure 4 Decay of Centerline Mean Velocity, $z/2r_o = 0.5$

tend to transform the "flat top" mean velocity profile, characteristic of an ideal jet, into profiles resembling a wall jet. Thus, the velocity at the nozzle centerline would be expected to decrease at a different rate for the jet/plate and jet/flap cases as compared to the unconfined case. For the $z/2r_o$ shown in this figure, the decrease in the mean velocity in x direction is exagerated by the fact that the flow has both changed direction and been "drawn down" toward the flap (C.F. Figures 5 and 6 in reference 2).

For $\lambda_j = 5.1$, the effectiveness of the flap in decelerating the flow in the x direction is apparent in Figure 4(a). The more rapid decay of the flow over the plate as compared to the unconfined jet is also noted. When $\lambda_j = 10.88$, the decay of the unconfined jet behaves quite similarly to the case for the smaller value of λ_j. The plate is slightly less effective in decelerating the flow while the effectiveness of the flap is reduced significantly.

The two observations that have been made concerning the relative rates of decay of the centerline mean velocity and the increase in the mixing widths for the flows over the flap with $\lambda_j = 5.1$ and $\lambda_j = 10.88$ are consistent and merit some discussion. The indication seems to be that as the value of λ_j gets larger and approaches the value corresponding to a free jet ($\lambda_j \rightarrow \infty$), the flap becomes less effective in both widening and decelerating the flow.

B. <u>Turbulent Intensities</u>

Turbulent intensity is the ratio of the rms turbulent velocity fluctuations to a reference mean velocity. In this investigation, turbulence level is non-dimensionalized by excess centerline mean velocity at the exit plane of the nozzle. The turbulent intensities are corrected for ambiguity noise using the method of Morton.[7]

In Figure 5, the turbulent intensity at $y/2r_o$ and $z/2r_o = 0.5$ is plotted versus downstream location, $x/2r_o$. For both $\lambda_j = 5.1$ and

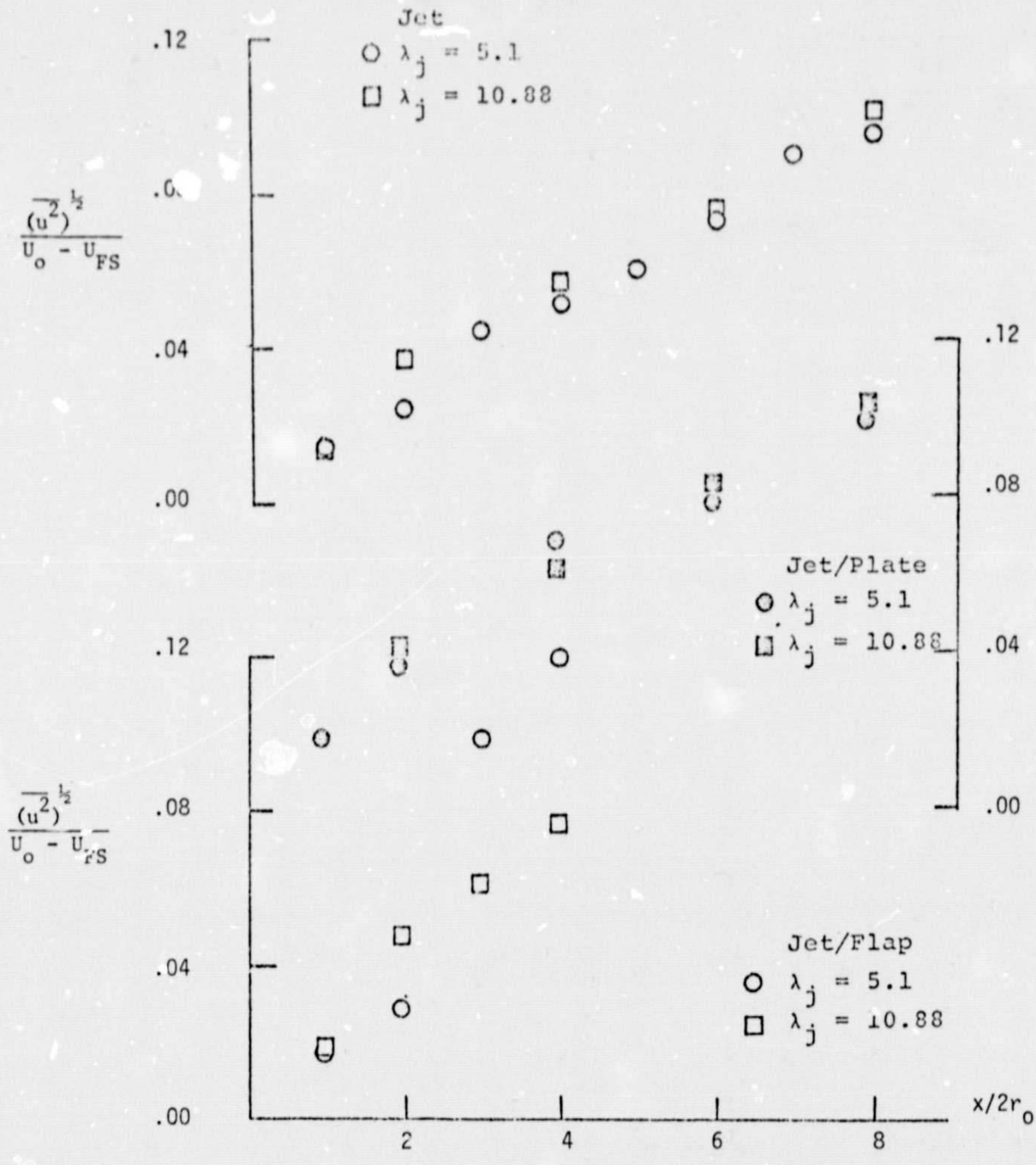

Figure 5 Growth of Turbulent Intensity, $\overline{(u^2)}^{1/2}$, at Centerline

$\lambda_j = 10.88$, the turbulence increases at about the same rate for both the unconfined coflowing jet and the flow over the plate. The magnitude is consistently higher for the plate configuration. In fact, λ_j seems to have very little effect on the experimental data.

For the flow over the flap, however, the value of the parameter, λ_j, is of considerable importance. In the case with $\lambda_j = 10.88$, the increase in turbulence is at a higher rate than is the case for the other two configurations. However, with $\lambda_j = 5.1$, this increase is much more rapid. This fact is quite consistent with the observations made concerning the decay of the mean velocity. At the location in the flow field where the jet is decelerated and widened at the most rapid rate, the turbulence is also amplified greatly giving a strong indication that the flap serves to quickly break-up the potential core flow.

C. Integral Scales*

The longitudinal integral time scale is defined as follows:

$$T_1 = \int_0^{t^*} \overline{u(t)\, u(t+t')}\; dt'$$

where t^* is the time at which the integral first reaches the value of zero.[8]

The growth of the integral time scale for the unconfined jet is addressed in Figures 6 (a) and (b). Figure 6 (a) is concerned with the centerline growth while 6(b) deals with the lateral location corresponding to the lip of the nozzle. At the lip of the nozzle, the integral time scale is found to grow linearly downstream. This is the same trend Lawrence [9] observed when measuring the integral length scale. The time scales for both

---

*Integral time scales are discussed here since the usual conversion to length scales using Taylor's hypothesis would not apply.

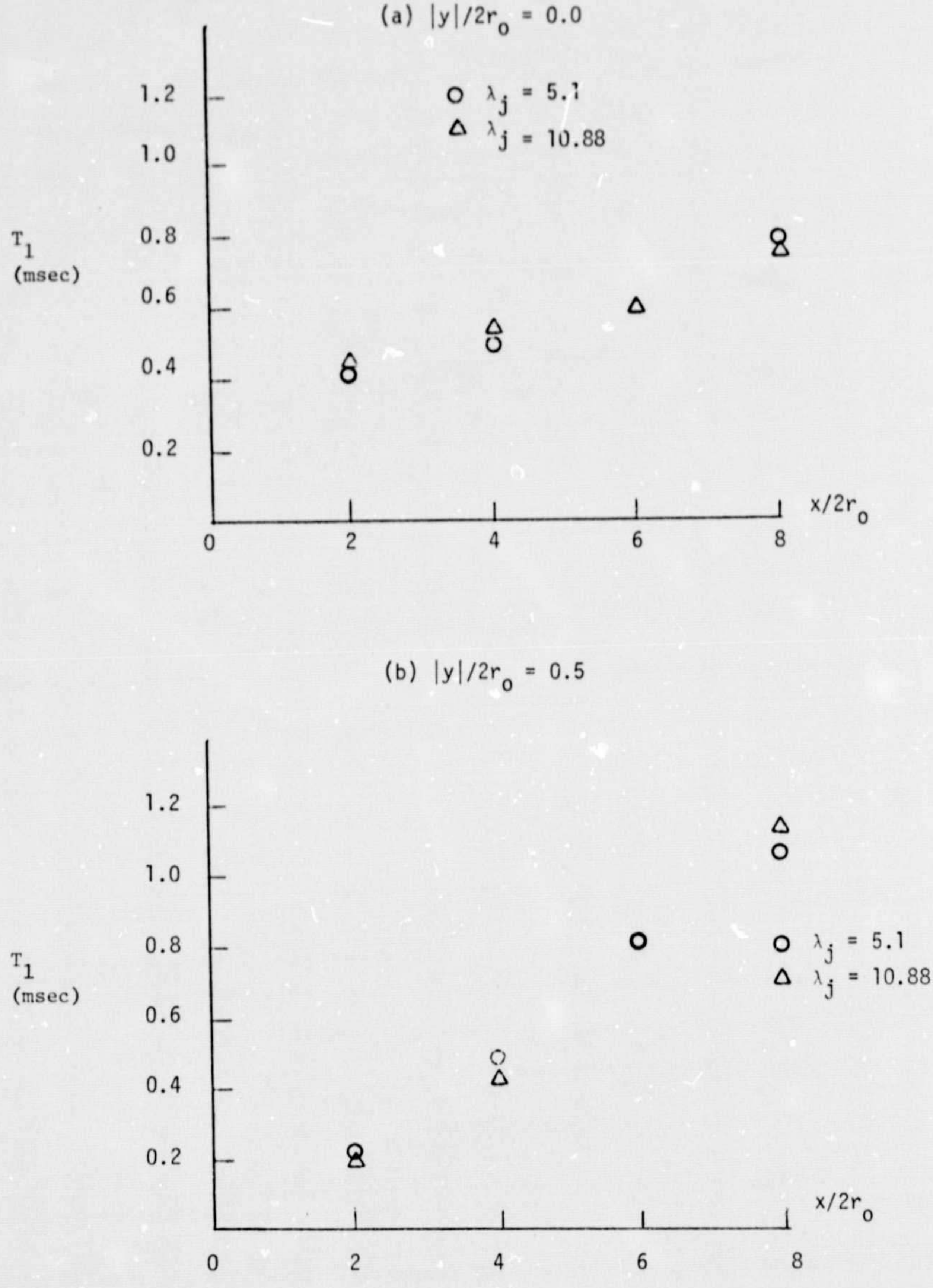

Figure 6 Development of Integral Time Scale for Jet, $z/2r_o$ = 0.5

velocity ratios grow at approximately the same rate. At the centerline of the flow field, the integral scale also grows similarly for both of λ_j. The implication is that the velocity of the outer tunnel flow does not have a significant effect on the turbulence for the first few diameters downstream.

For the flow over the flap, the development of the integral time scale is quite different than is the case for the coflowing jet (Figure 7). The values of the integral scale increase rapidly the first two diameters downstream but then remain fairly constant ($|y|/2r_o = 0.5$) or actually slightly decrease ($|y|/2r_o = 0$). It should also be noted that the value for the velocity ratio, λ_j, does not seem to have a significant effect on the time scale.

The growth of the integral scales for the flow over the plate is presented in Figure 8(a) and (b). For $|y|/2r_o = 0.5$, the integral scale at the larger velocity ratio is consistently larger in magnitude than it is for $\lambda_j = 5.1$.

D. Pressure-Velocity Correlations

Additional information concerning the turbulence structure of the various flow fields can be gained from measurements of the pressure fluctuations at both the wall and in the turbulent jet and correlating those signals with fluctuating turbulent velocities in the potential core and in the shearing region.

Pressures are measured either at surface ports located on the flap or plate or by a pressure probe in the flow. In either case, the following space-time correlation are measured:

$$R_{pa}(\vec{x}, \vec{\xi}, t, \tau) = \frac{\overline{P(\vec{x},t)u(\vec{x} + \vec{\xi}, t + \tau)}}{[\overline{p(\vec{x},t)^2}]^{\frac{1}{2}}[\overline{u(\vec{x},\vec{\xi},t + \tau)^2}]^{\frac{1}{2}}}$$

where $\vec{\xi}$ is the position of the velocity "probe", measured relative to the pressure probe and p is the static pressure measured at the wall or in the flow field.

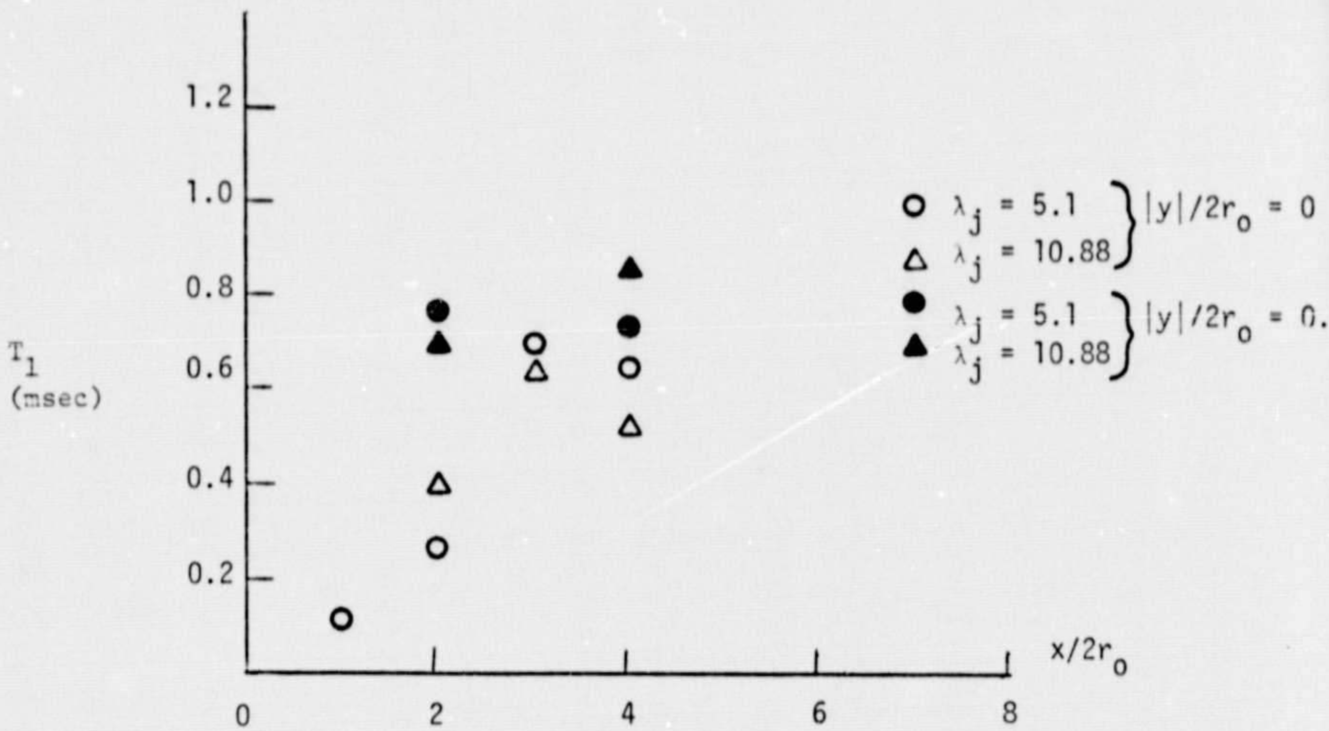

Figure 7 Development of Integral Time Scale for Jet/Flap $z/2r_o = 0.5$

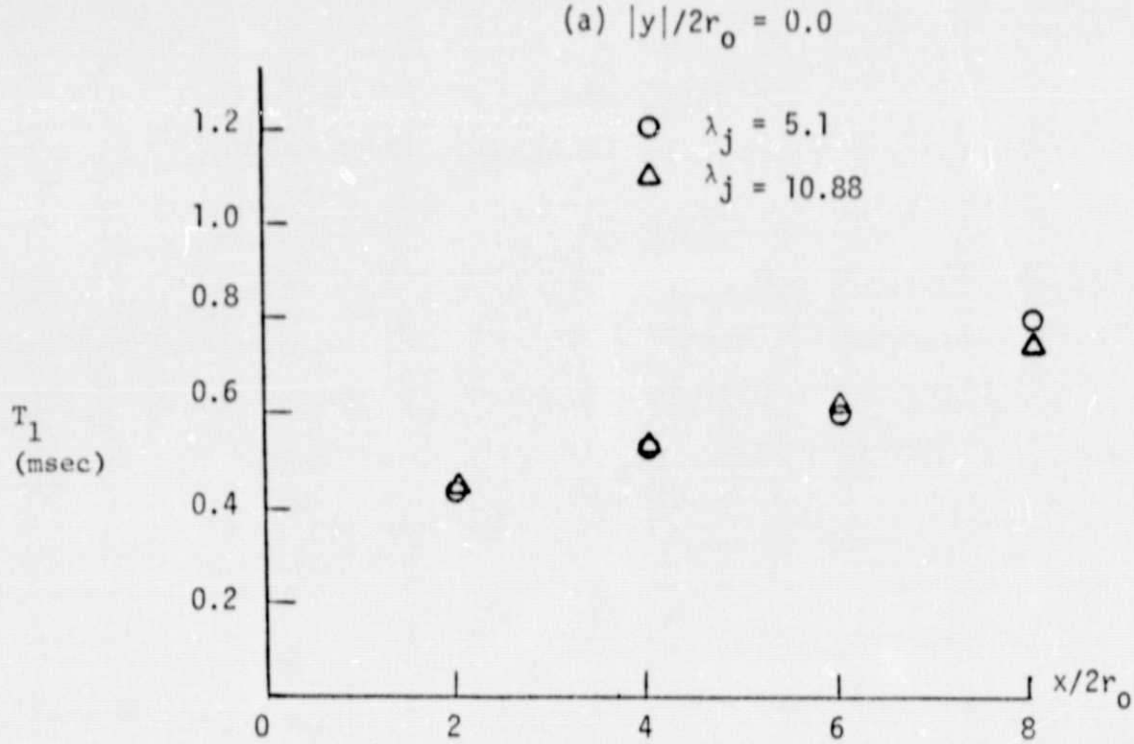

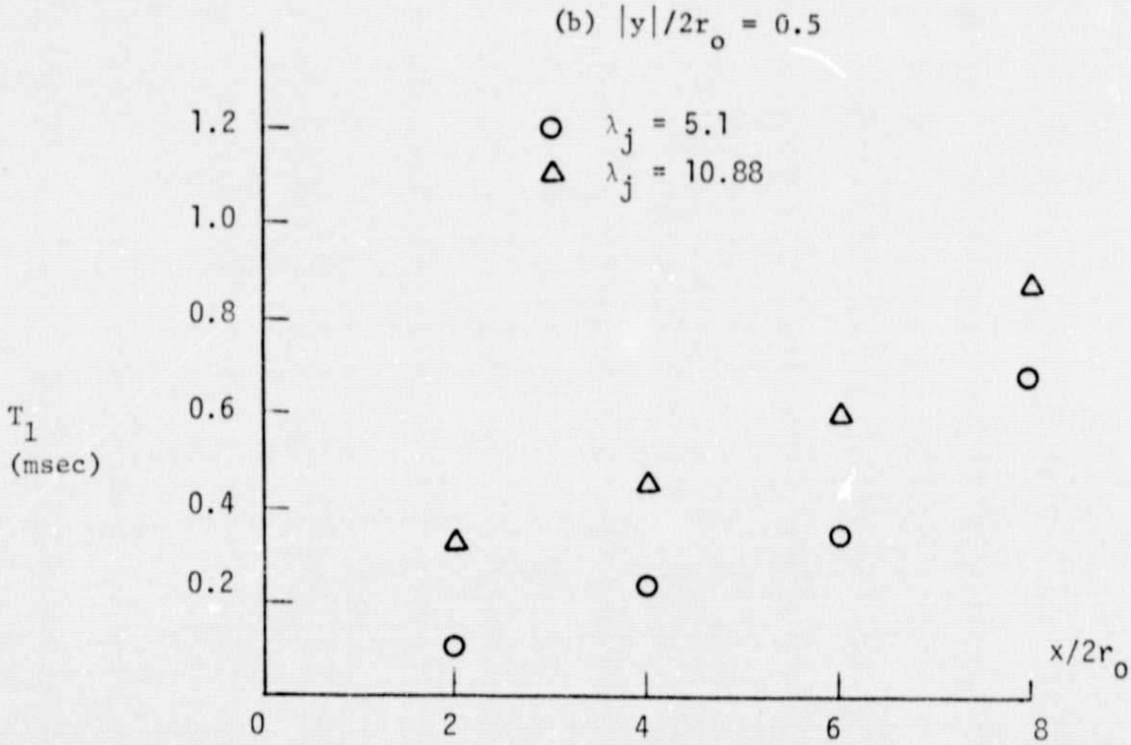

Figure 8 Development of Integral Scale for Jet/Plate, $z/2r_o = 0.5$

The primary focus of this segment of the experimental investigation is to determine the relationship between the pressure and the velocity fields. To show the dependence between the two fields, the coherence is plotted for various pressure and velocity monitoring locations. Coherence, which can be considered a correlation coefficient which varies with frequency, is defined as follows:

$$\delta_{12}{}^2 = \frac{|G_{12}|^2}{G_{11}G_{22}}$$

where G_{11}, G_{22} are the Fourier Transforms of the individual autocorrelation functions and G_{12} is the Fourier Transform of the cross-correlation function.

1. Wall Pressure Fluctuateans

Cross correlations between fluctuating pressure signals measured at surface ports in the plate and flap and turbulent velocity signals monitored at various locations in the flow field are determined.

Consider first the case of the flow over the plate. To clarify the relationship between pressure and velocity fluctuations, power spectral densities and coherence are determined with the laser "probe" at $\xi_3/2r_o = 0.2, \xi_1/2r_o = \xi_2/2r_o = 0$. Examples of the results for $x/2r_o = 4$ are shown in Figures 9-11.

Here the lateral positioning of the pressure port and laser probe varies from $|y|/2r_o = 0$ to $|y|/2r_o = 1$. It is found that inside the lip of the nozzle, $|y|/2r_o <= 0.5$ the velocity spectra and pressure spectra are characterized by large peaks at, in this instance, approximately 300 Hz. The coherence between the pressure and velocity signals is clearly the strongest at this peak frequency. As the pressure and velocity monitoring "probes" are moved outward from $|y|/2r_o = 0.5$ the spectral peaks are attenuated and the resultant decrease in the coherence is noted.

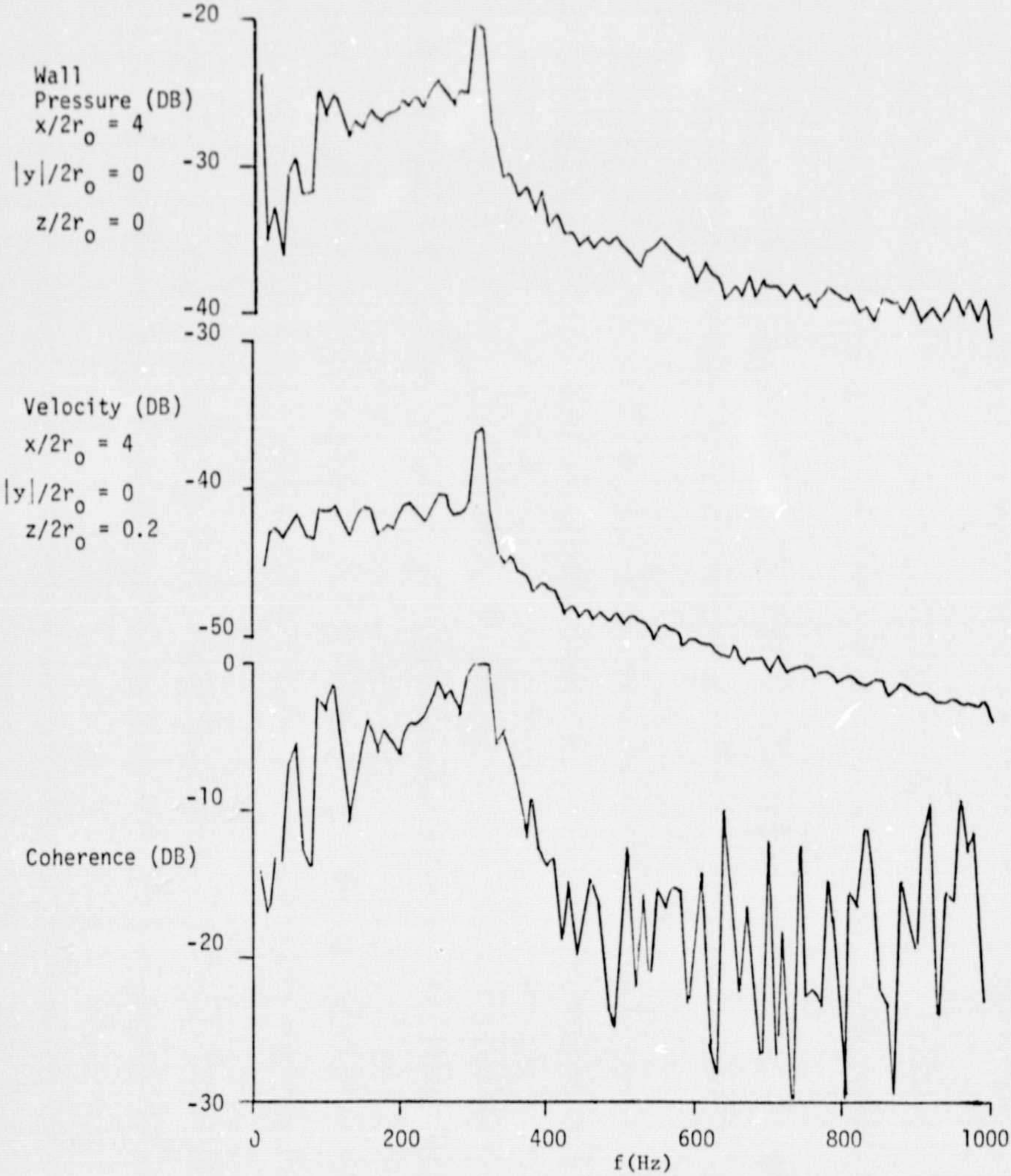

Figure 9 Wall Pressure and Velocity Spectra, and Coherence-Jet/Plate $\xi_3/2r_o = 0.2$ ($\lambda_j = 5.1$, DB referred to Dynamic Pressure/Hz)

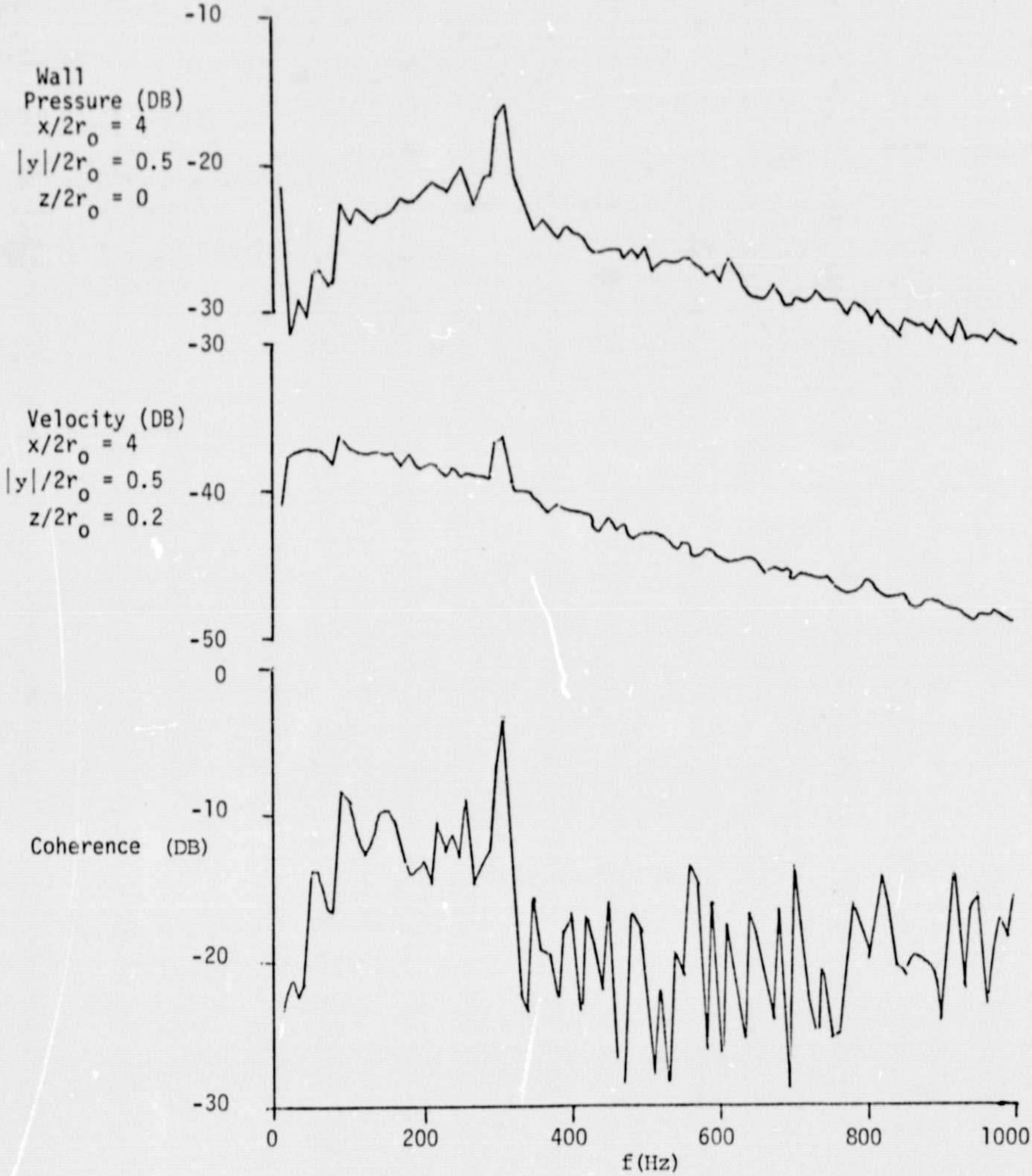

Figure 10 Wall Pressure and Velocity Spectra and Coherence - Jet/Plate $\xi_3/2r_o = 0.2$ ($\lambda_j = 5.1$, DB referenced to Dynamic Pressure/Hz)

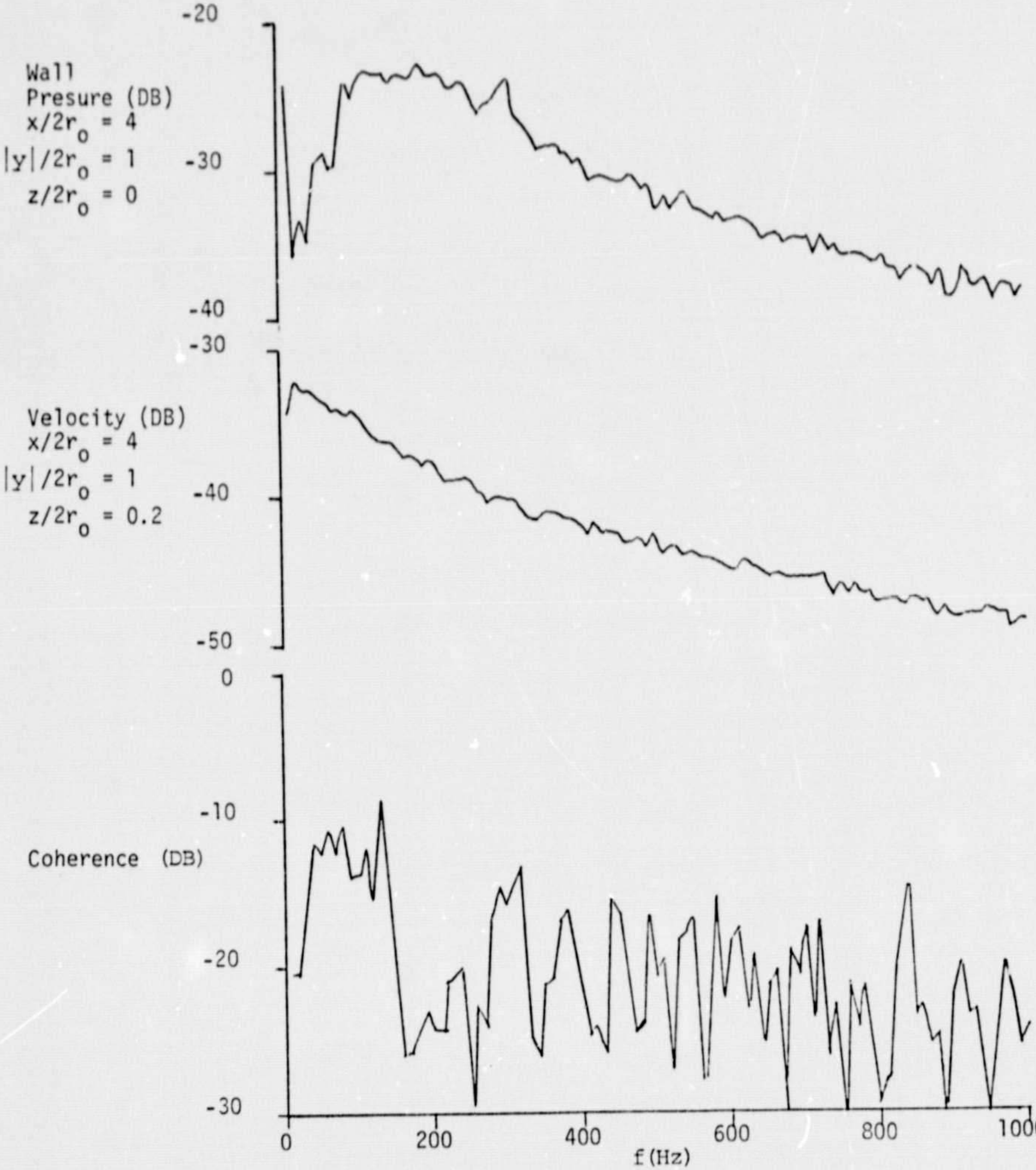

Figure 11 Wall Pressure and Velocity Spectra and Coherence - Jet/Plate $\xi_3/2r_o = 0.2$ ($\lambda_j = 5.1$, DB referenced to Dynamic Pressure/Hz)

Coherences are also determined for the flow over the plate with $\xi_2/2r_o$ varying from 0 to 1, $\xi_1/2r_o = 0$ and $\xi_3/2r_o = 0.5$ (Figure 12). Physically, the laser control volume is held fixed at the location $x/2r_o = 4$, $|y|/2r_o = 0$, and $z/2r_o = 0.5$ with the fluctuating velocity signal being correlated with surface pressures measured at $x/2r_o = 4$, $z/2r_o = 0$, and $|y|/2r_o = 0$, 0.5 and 1. Though not shown here, it is found that the velocity spectra are not as peaked as is the case at $z/2r_o = 0.2$ and, hence, the coherence between the pressure and velocity signals is diminished. Note that the coherence decreases as the surface probe is moved laterally outward from the jet centerline.

For the flow over the flap, coherences are determined between the pressures monitored at the surface and the velocities at the $|y|/2r_o = 0$ location. The downstream location is held fixed at $x/2r_o = 4$. In Figure 13, coherences are shown with the laser "probe" held fixed at $|\xi_2|/2r_o = 0$ and $z/2r_o = 0.2$ while in Figure 14, the laser measuring volume is located at $|y|/2r_o = 0$ and $z/2r_o = 0.5$. Many of the same observations that were made concerning the flow over the plate can be made once again. The velocity spectra are found to be much more peaked closer to the surface of the flap. The coherence is larger in magnitude between the wall surface pressure and the velocity fluctuations with $\xi_3/2r_o = 0.2$. Also, the coherence is the strongest at approximately 300 Hz.

2. Pressure Fluctuations at Probe

Cross correlations and coherences are determined between the static pressure measured by a static pressure probe and the turbulent velocity fluctuations measured at the jet axis. The pressure is monitored at three lateral locations (i.e., $|y|/2r_o = 0, 0.5, 1.0$) with the velocity control volume remaining fixed. The vertical location for the pressure probe and LDV volume remains fixed at $z/2r_o = 0.5$.

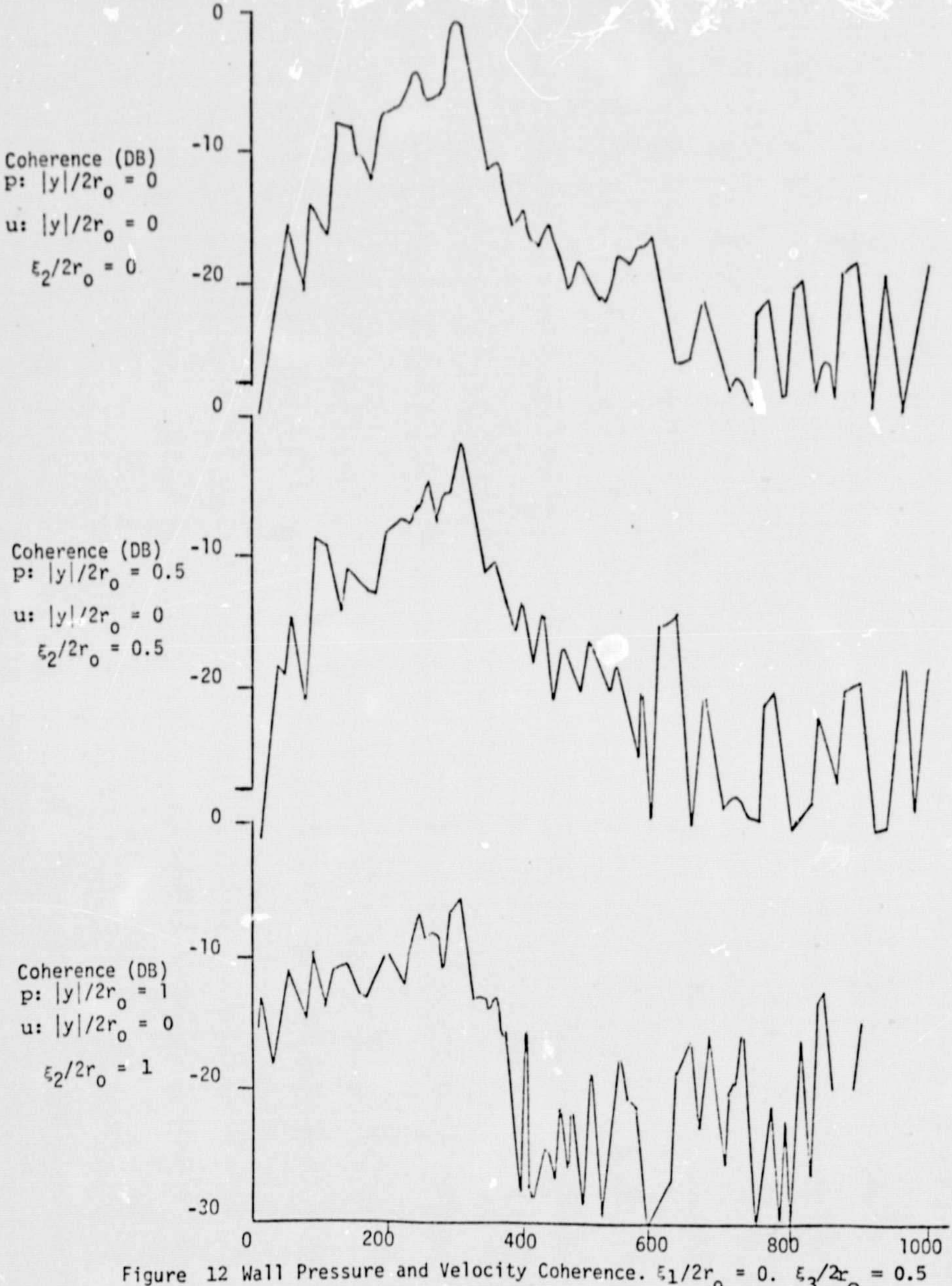

Figure 12 Wall Pressure and Velocity Coherence. $\xi_1/2r_o = 0.$ $\xi_3/2r_o = 0.5$
Jet/Plate (λ_j = 5.1, DB referenced to Dynamic Pressure/Hz)

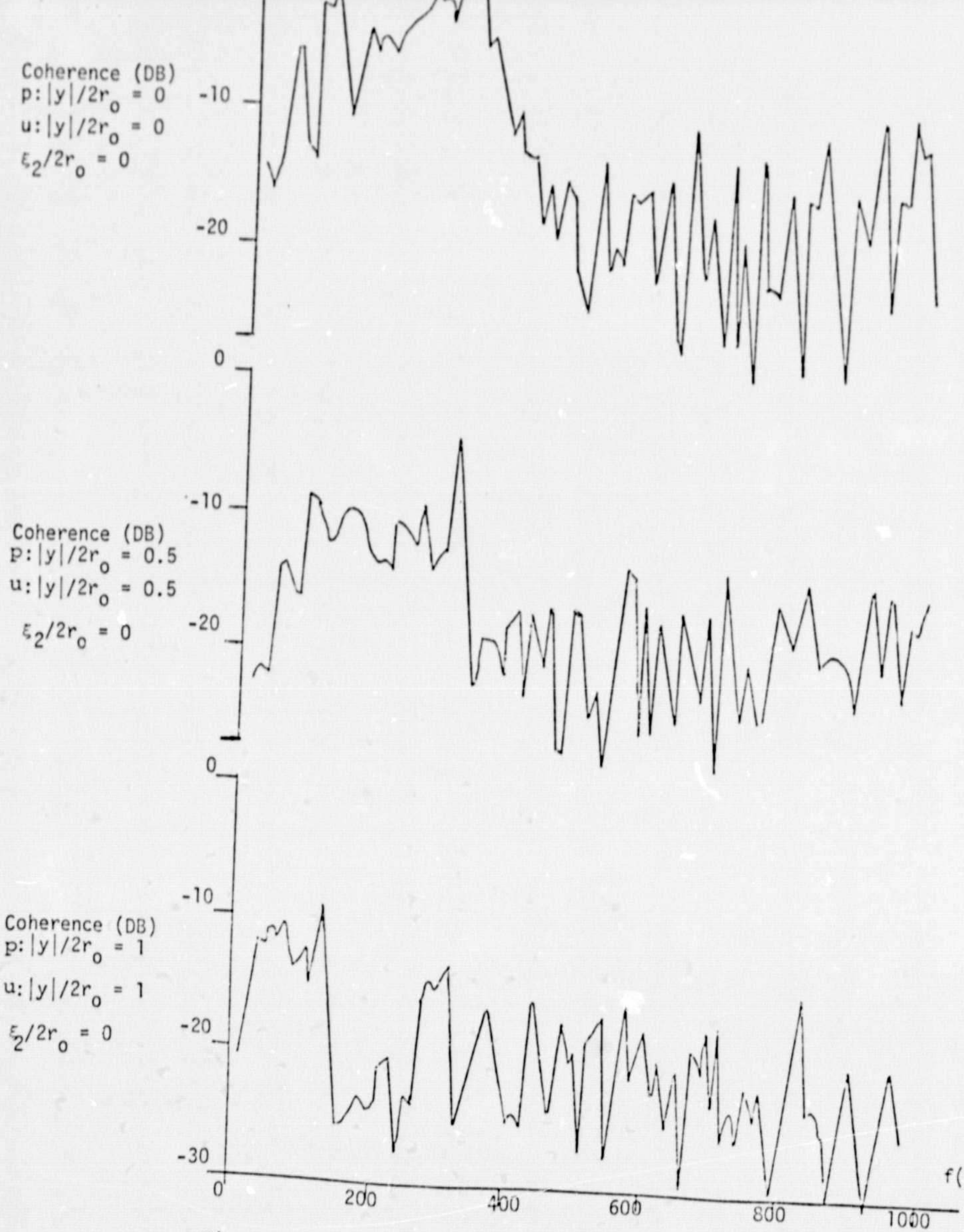

Figure 13 Wall Pressure and Velocity Coherence, $\xi_1/2r_o = 0$, $\xi_3/2r_o = 0.2$ Jet/Flap ($\lambda_j = 5.1$, DB reference to Dynamic Pressure/Hz)

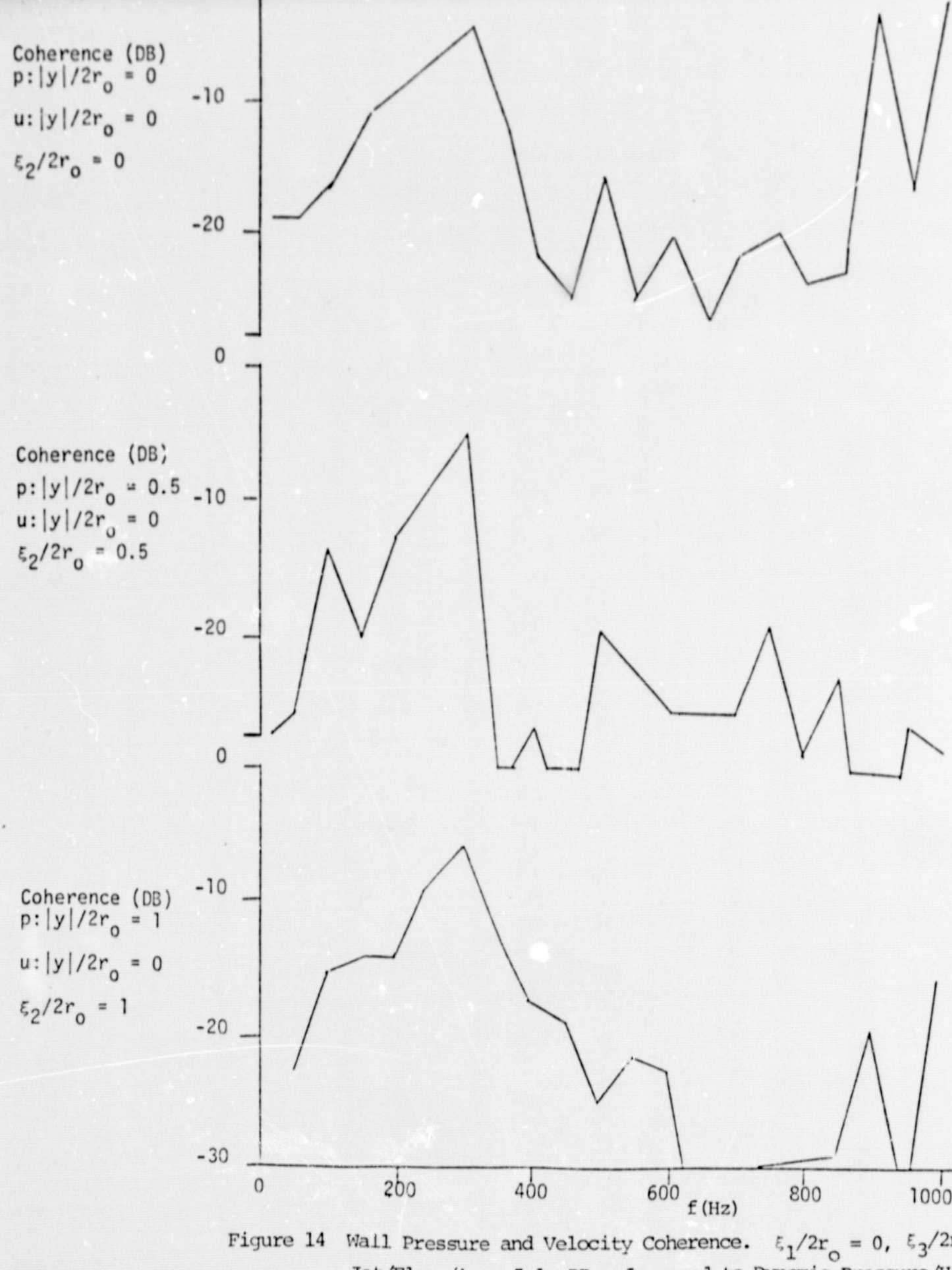

Figure 14 Wall Pressure and Velocity Coherence. $\xi_1/2r_o = 0$, $\xi_3/2r_o = 0.5$ Jet/Flap ($\lambda_j = 5.1$, DB referenced to Dynamic Pressure/Hz)

For the unconfined, coflowing jet, the coherences between the fluctuating pressure and velocity signals are shown in Figures 15-17 for the downstream location, $x/2r_o = 4$. In Figure 15, power spectral densities as well as the coherence between the pressure and velocity field are presented with $\xi_2/2r_o = 0$. Notice that the spectra and the coherence peak at approximately 300 Hz, as was the case for the pressure measured at the wall. In Figures 16 and 17, as the pressure probe is moved radially outward, the coherence decreases.

Next, consider the case of the turbulent jet flowing over the flat plate for the downstream location, $x/2r_o = 4$. The pressure spectrum is again found to be markedly peaked at 300 Hz at $|y|/2r_o = 0$ and this "bump" is both broadened and attenuated out from the jet axis. The velocity spectrum is not as peaked as it is the case of the unconfined jet. The coherence of the two fluctuating signals (Figure 18) has been significantly reduced with the plate in the flow field, and it decreases with increasing lateral separation of the pressure probe and the laser control volume. The coherences obtained from the turbulent jet/flap configuration for the downstream location $x/2r_o = 4$ are shown in Figure 19. The peak in the velocity spectra has been virtually eliminated. It is interesting to compare the coherence of each $\xi_2/2r_o$ position for this flow with the jet/plate and unconfined jet flow fields. The coherences for the two confined jet flows are quite close in magnitude. The transformation of the turbulent jet into either a classical wall jet or curved wall jet does decrease the relationship between the fluctuating pressure and velocity fields.

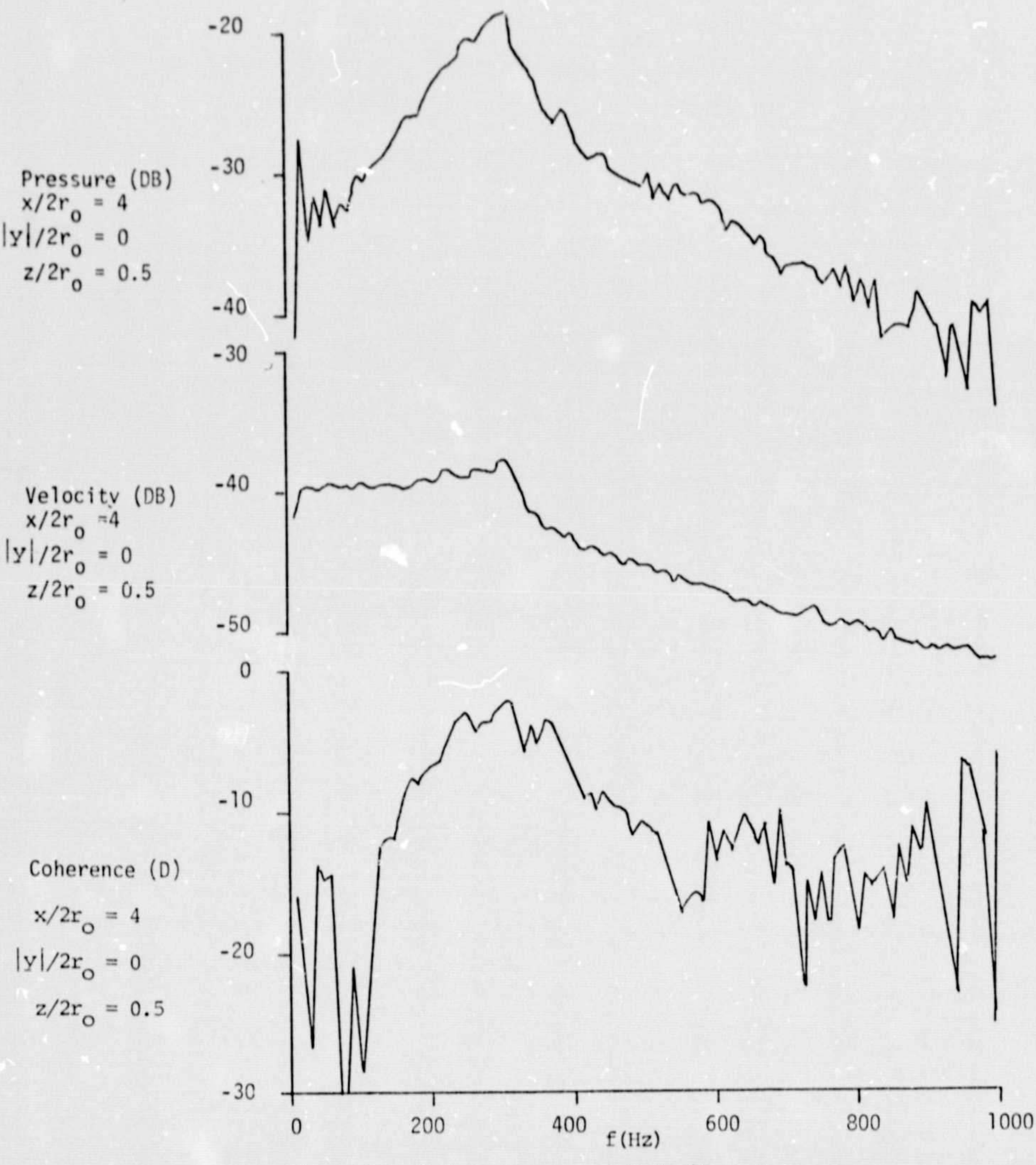

Figure 15 Wall Pressure and Velocity Coherence $\xi_1/2r_o = 0$, $\xi_2/2r_o = 0$, $\xi_3/2r_o = 0$. Jet ($\lambda_j = 5.1$, DB referenced to Dynamic Pressure/Hz)

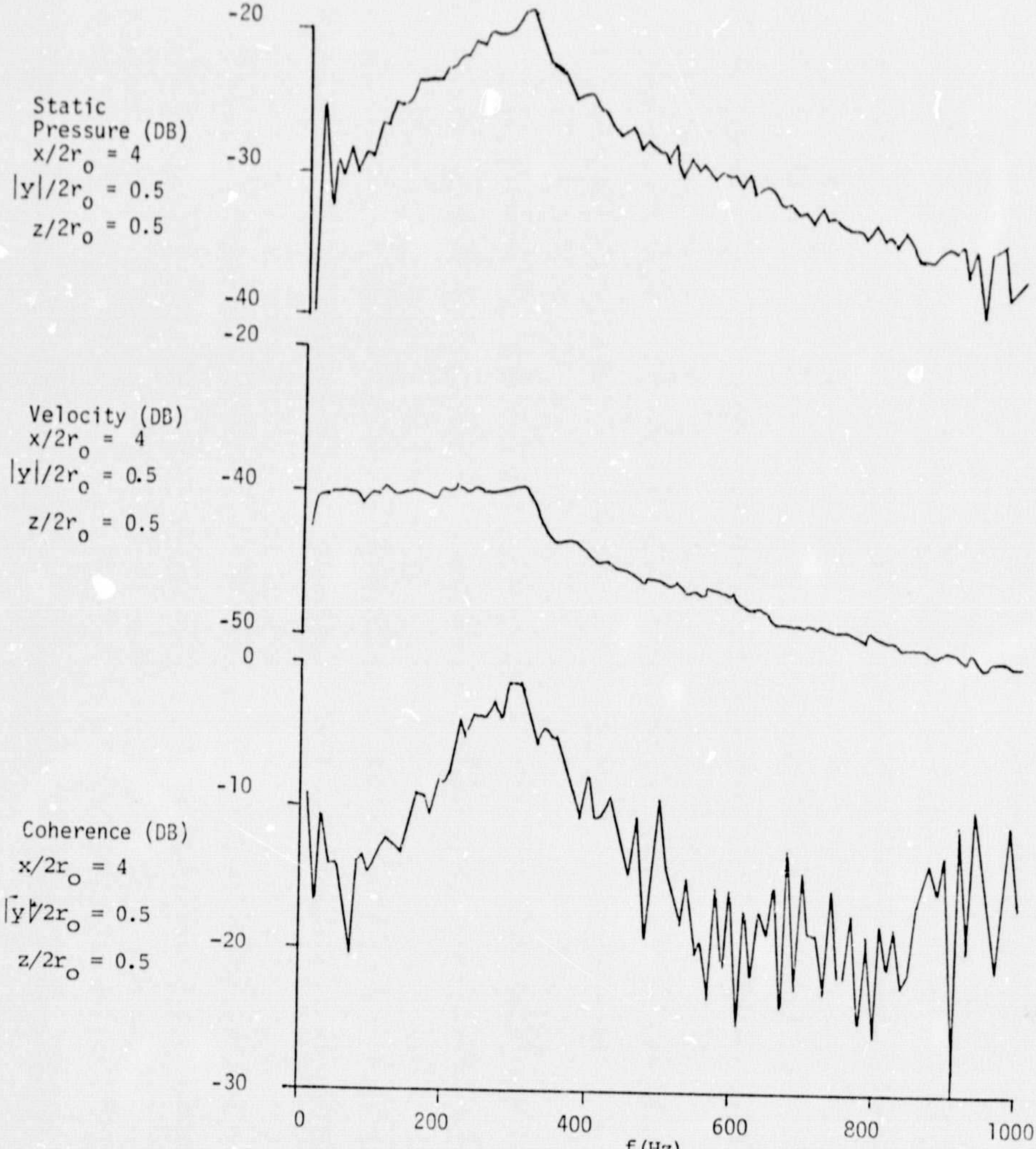

Figure 16 Wall Pressure and Velocity Coherence
$\xi_1/2r_o = 0$, $\xi_2/2r_o = 0$, $\xi_3/2r_o = 0$. Jet
($\lambda_j = 5.1$, DB referenced to Dynamic Pressure/Hz)

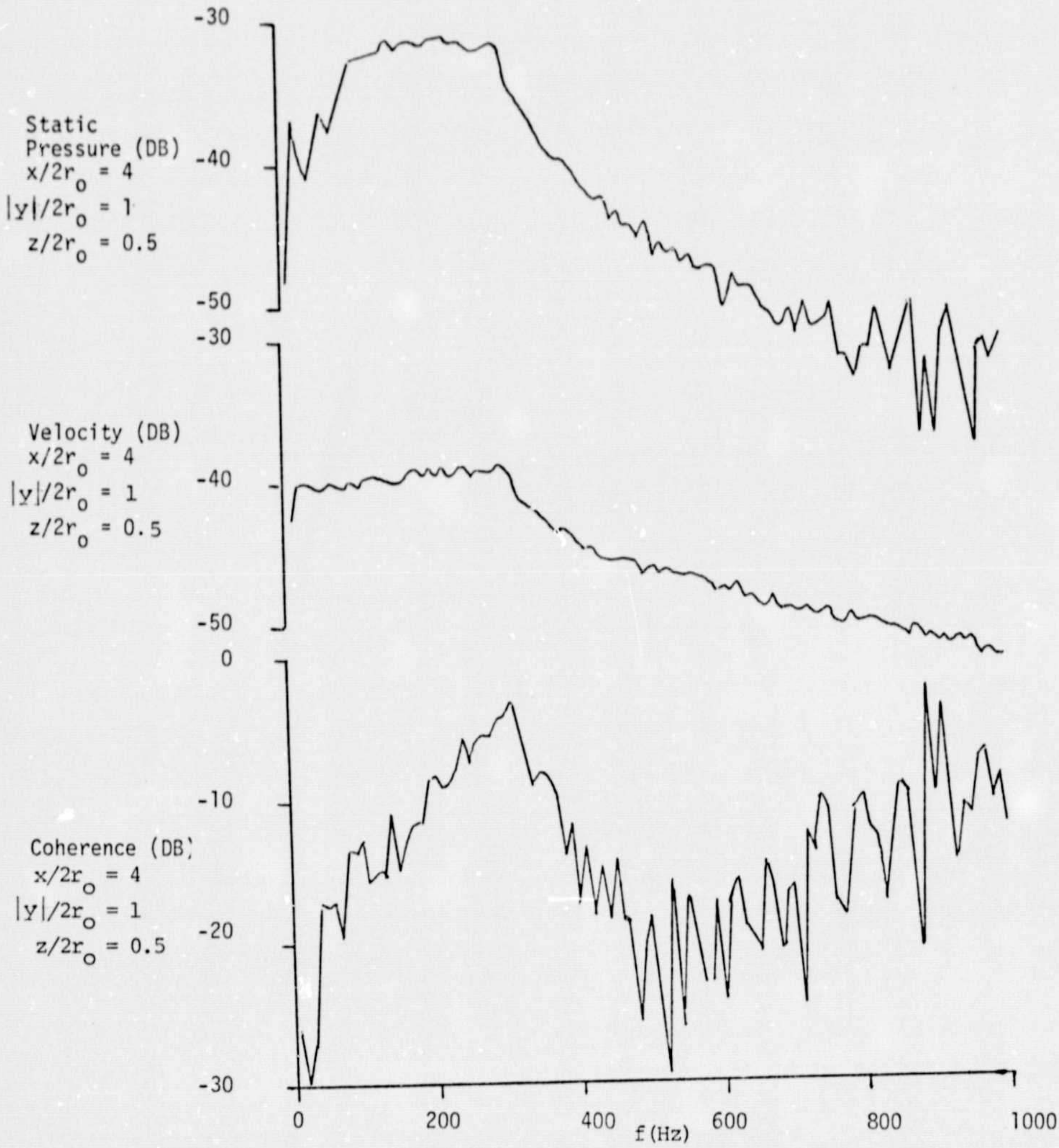

Figure 17 Wall Pressure and Velocity Coherence
$\xi_1/2r_o = 0$, $\xi_2/2r_o = 0$, $\xi_3/2r_o = 0$. Jet
($\lambda_j = 5.1$, DB referenced to Dynamic Pressure/Hz)

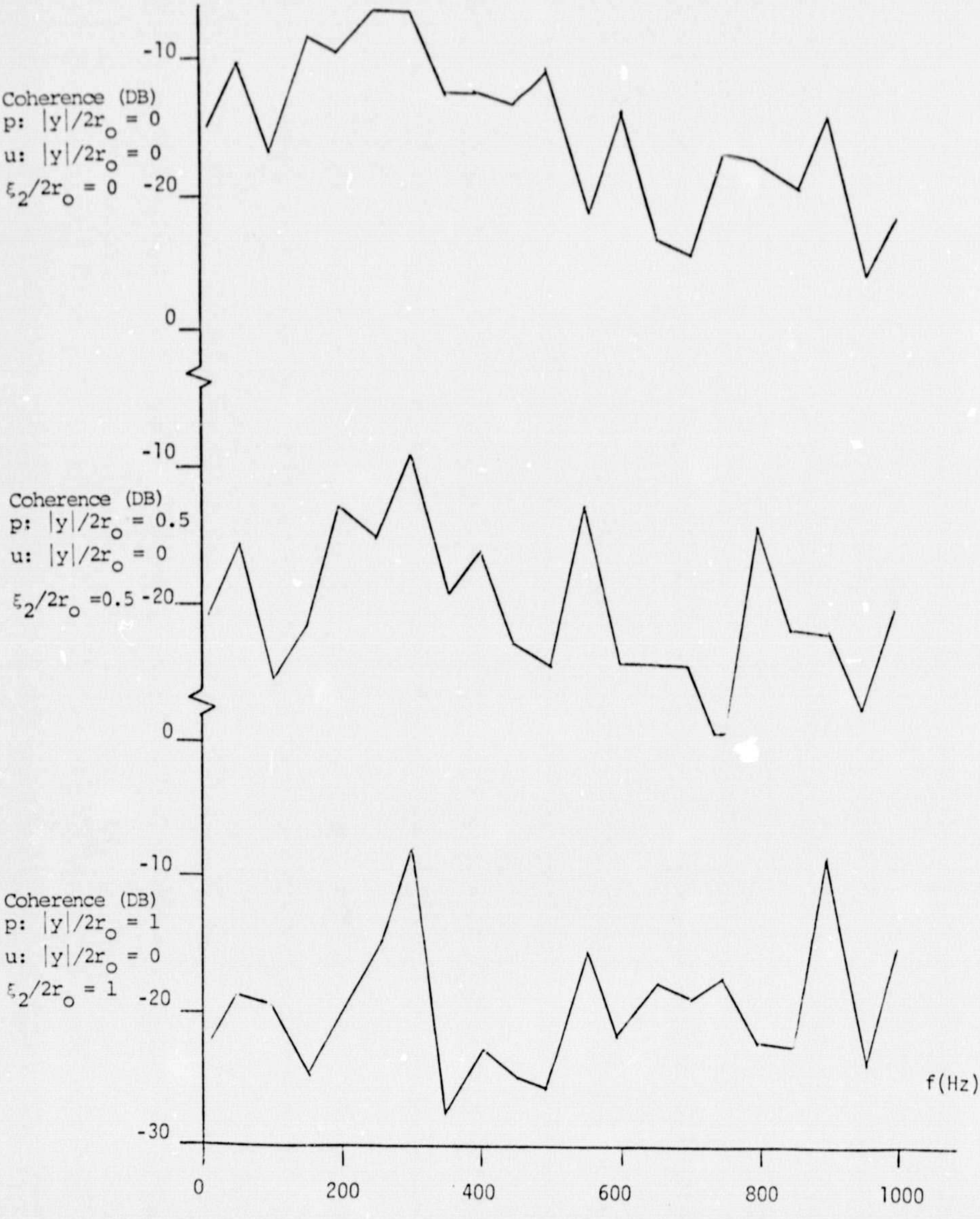

Figure 18 Static Pressure and Velocity Coherence. $\xi_1/2r_o = 0$, $\xi_3/2r_o = 0$. Jet/plate ($\lambda_j = 5.1$, DB referenced to Dynamic Pressure/Hz)

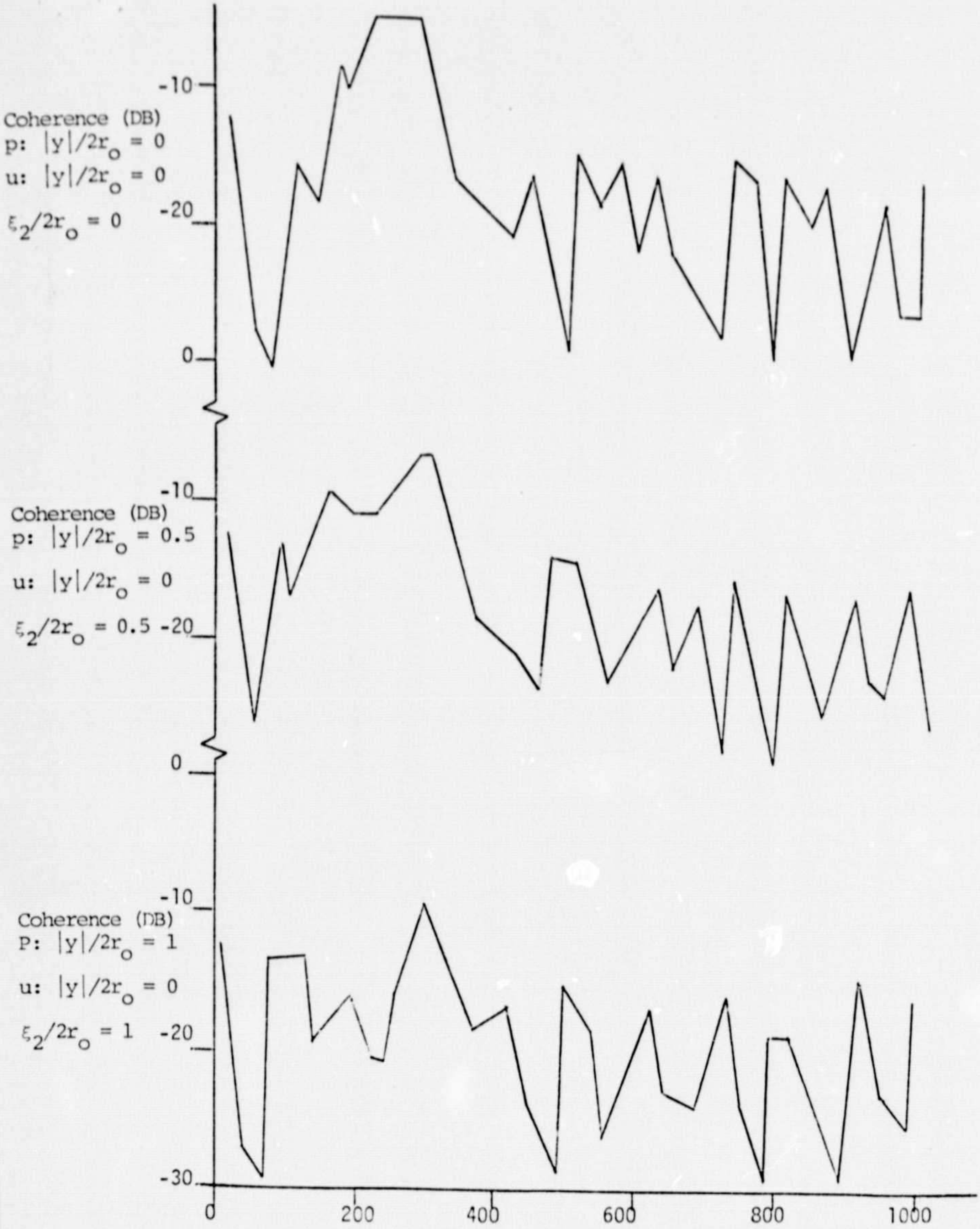

Figure 19 Static Pressure and Velocity Coherence. $\xi_1/2r_o = 0$, $\xi_3/2r_o = 0$, Jet/Flap ($\lambda_j = 5.1$, DB referenced to Dynamic Pressure/Hz)

IV SUMMARY

The value of the velocity ratio, λ_j, was found to have a significant influence on the mean velocity field. For the case of the flow over the flap, an increasing value of λ_j decreased the effectiveness of the curved wall surface in diminishing the x-directed momentum. Evidence existed that as λ_j approached infinity, the flow would not remain attached. The parameter λ_j influenced the width of the mean velocity profiles, as well, especially in the case of the flow over the flap. An increase in λ_j caused a resultant decrease in the mixing width, y_m.

Pressure velocity correlations using both the static pressure probe and the surface ports yielded strong evidence that as the flow progresses downstream, and the flow becomes a fully developed turbulent flow, the relationship between the pressure and velocity field diminishes. For the first several diameters downstream from the exit plane when the pressure and velocity spectra peak at approximately 300 Hz, the coherence between the two fluctuating fields is the strongest.

V ACKNOWLEDGEMENT

This work was supported in part by NSF under grant 7522488 and NASA under grant NGR 47-005-219-3.